The International Journal of Advanced Manufacturing Technology (2022) 122:1467–1478
https://doi.org/10.1007/s00170-022-09986-4

ORIGINAL ARTICLE

Determination of local density in components made by fused deposition modeling through indentation test

Francesco Lambiase[1] · **Silvia Ilaria Scipioni**[1] · **Alfonso Paoletti**[1]

Received: 25 May 2022 / Accepted: 12 August 2022 / Published online: 23 August 2022

Abstract
The present study is aimed at determining the local density of components made by fused deposition modeling (FDM) through non-destructive indentation tests. An experimental campaign was performed to assess such a relationship. Specimens were made varying the amount of material flow and the direction of deposition. The specimen's dimension and weight were measured to determine the average density. The internal porosity due to uncomplete filling produced due to the deposition process was also assessed through cross-sectioning. Instrumented indentation tests were conducted on the samples to determine a relationship between the density and the slopes during the loading and unloading phases. The tests were performed using flat cylindrical indenters of different diameters. The results indicated that the density of the specimens was strongly influenced by the adopted material flow and the orientation during deposition. An empirical relationship was determined between the slopes measured during indentation tests and the density. Such a relationship is independent of the deposition orientation. The optimized procedure represents a valuable tool to determine the local density of components made by fused deposition modeling through non-destructive indentation tests.

Keywords Additive manufacturing · Fused deposition modeling · Material extrusion · Characterization · Mechanical testing · Quality assessment

1 Introduction

Additive manufacturing (AM) processes are achieving growing interest within the scientific community and industrial companies [1–3]. Since the early application of these processes for rapid prototyping purposes, additive manufacturing has been rapidly extended to rapid tooling. The challenge is to use AM to provide an alternative solution for the rapid fabrication of final products. However, applying these processes to finished manufacturing products introduces new issues. The components' mechanical properties are different from parts made by traditional methods (e.g., injection molding for plastics) [4]. This is due to the inherent growing mechanism (layer by layer) of the finished part that can be seen as an aggregate of different bonded layers. Furthermore, with few exceptions (e.g., sheet lamination), additive manufacturing processes involve many porosities. This is particularly evident in components made by material extrusion processes such as fused deposition modeling (FDM) since the great dimension of the raw material involved in this process and the semi-solid state of the material during the deposition.

The presence of the porosities influences the behavior of the components made by additive manufacturing processes. Porosities reduce the load-bearing area and induce severe stress concentration leading to higher stress. As explained above, compared to other additive manufacturing processes, the process-induced porosities in the fused deposition modeling (FDM) process are even more challenging. Indeed, during the FDM process, a relatively low pressure (as compared to conventional manufacturing processes such as injection molding) is applied to the molten material flowing from the nozzle to the underlying layer. This hinders the complete filling of the volume and adhesion with side and underlying layers, leading to continuous porosities within the component. Therefore, fused deposition modeling (FDM) parts show anisotropic plastic behavior [5]. This also causes the

✉ Francesco Lambiase
francesco.lambiase@univaq.it

[1] Dept. of Industrial and Information Engineering and Economics, University of L'Aquila, Zona Industriale Di Pile, Monteluco Di Roio, via G. Gronchi 18, 67100 L'Aquila (AQ), Italy

fracture mechanism and elongation at rupture to be strongly influenced by the direction of the load with respect to the growing direction [6]. The porosities also affect the crystallinity of semi-crystalline materials such as polylactide acid (PLA), as reported in [4].

Compared to conventional manufacturing processes, FDM is also less standardizable; the deposition condition, the adhesion between the deposited filament, and the shape and dimensions of the porosity depend on the tool path. Thus, the mechanical properties are also influenced by the component's geometry. This further complicates the characterization of the components and the prediction of the behavior of the components. This limits the adoption of testing samples that represent the manufacturing conditions of the actual part. This is due to the thermal history of the material that flows from the nozzle, which also depends on the thermal diffusion with the surrounding material. Furthermore, in the FDM process, the accelerations/decelerations in the proximity of rapid direction changes also determine the material's uneven "distribution."

In the FDM process, the typical dimension of the extruder, which determines the dimension of the deposited filament, ranges between 0.3 and 0.6 mm. These values are one order of magnitude higher than the size of the powder used in powder bed fusion processes of plastics. Consequently, the porosities in FDM are larger than those observed in other AM processes such as powder bed fusion and binder jetting. Compared to stereolithography, the viscosity of the material during the extrusion is higher than that of photopolymers, leading to larger porosities as well. Thus, the presence and dimensions of porosities in FDM are generally more challenging than other additive manufacturing processes of plastics. The characterization of porosities can be precisely conducted through X-ray computed tomography analysis [7]. This approach enables the measurement of the location, the arrangement, and the dimension of the porosities, through a digital twin of the actual component. However, computed tomography analysis involves expensive testing equipment and a long scanning time that limits the applicability of such a testing technique. On the other hand, the application of non-destructive testing such as indentation tests could provide some more insight into the local behavior of the component with a reasonable analysis time. For these reasons, the adoption of non-destructive testing (NDT) performed on actual components would significantly improve the quality assessment of the parts [8, 9]. For instance, indentation tests have been investigated to predict the mechanical behavior of metals and plastics [10]. Indentation tests were used for testing the mechanical properties of components made by direct energy deposition (DED) [11], and binder jetting [12].

So far, indentation tests have been applied to materials showing relatively small porosities, generally much smaller than those observed in parts made by FDM. This enabled the adoption of typical hardness indenters and even nanoindentation tests to determine the characteristics of the tested material. Such procedures and tools are not suitable for testing parts made by FDM since the indenter is much smaller than the porosities of the part. Therefore, the present work aims to develop a procedure and tools to determine the porosity of components made by FDM through an instrumented indentation test. This was performed experimentally by producing samples with different densities. The density of the components was determined through other measuring techniques to establish a relationship between the characteristic slopes determined in indentation tests and the porosity.

2 Materials and methods

The experimental campaign was conducted on rectangular specimens made of polylactide acid (PLA) produced by Fabbrix. PLA has widespread application, inherent recyclability, and reduced cost compared to other plastics [13]. The samples were parallelepiped-shaped with 5 mm × 60 mm × 20 mm, and were fabricated using a commercial FDM machine model Ender-6 by Creality. This machine enables the selection of a wide range of parameters and deposition conditions. During the deposition process, the extruder and the bottom plate temperature were set at 210 °C and 60 °C, respectively. A deposition rate of 4000 mm/min was selected. A layer thickness of 0.2 mm was selected. This value represents 50% of the nozzle diameter ($d = 0.4$ mm) used for deposition. The samples were filled using five perimetral shells with a fixed width of 0.5 mm. The software Simplify 3D was used to control all the deposition settings. Different extrusion multipliers (94%, 97%, 100%, 103%, and 106%), which determine the amount of material flow during the deposition, were adopted to produce specimens of different porosities. The samples were produced using two deposition strategies, vertical and horizontal, as depicted in Fig. 1. Three replicates were made for each deposition condition.

After printing, the weight of the specimens was measured through a precision balance model XT1220M by Precisa, and the main dimensions were measured. This enabled us to determine the density produced through different extrusion multipliers.

The samples were cross-sectioned following standard metallographic procedures, as schematized in Fig. 2. The portions were molded into resin, and polished with fumed silica suspension 0.2 mm. Finally, the samples were treated in an ultrasonic bath to remove material from the porosities. The samples were thus observed using a digital stereoscope model M205 by Leica.

Instrumented indentation tests were carried out using MTS's Universal Testing Machine model C43.50. The

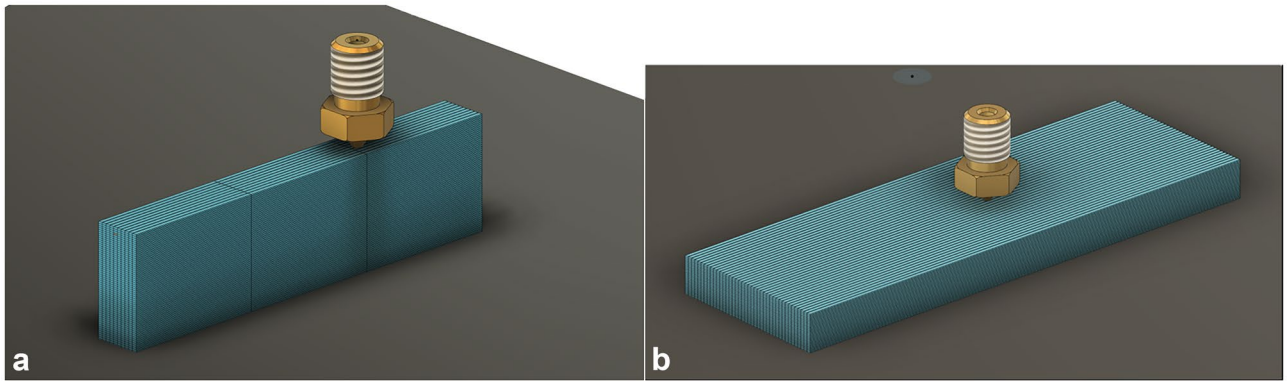

Fig. 1 Schematics of **a** vertical and **b** horizontal disposition of the samples during FFF deposition

specimen was positioned horizontally (with the 20×20 surface perpendicular to the indenter) on a compression plate. A cylindrical indenter was placed on the upper side of the sample, as shown in Fig. 3a. Indentation tests were conducted using cylindrical indenters with different diameters: $D = 2$ mm and $D = 4$ mm, at a constant travel speed of 1 mm/min, as depicted in Fig. 3b. The test was divided into two phases: the loading phase until the tool traveled for 0.6 mm through the sample thickness and the unloading phase, which involved a reverse tool direction. The tool travel depth was selected based on the previous experimental test.

The force–displacement curves were recorded during the loading and the unloading phases; then, the curves were elaborated using an algorithm within the MATLAB 2021a environment. The algorithm identifies the linear path of the curves during the loading and unloading phases and identifies the slopes (E_1 and E_2, respectively) of each path, as shown in Fig. 3b.

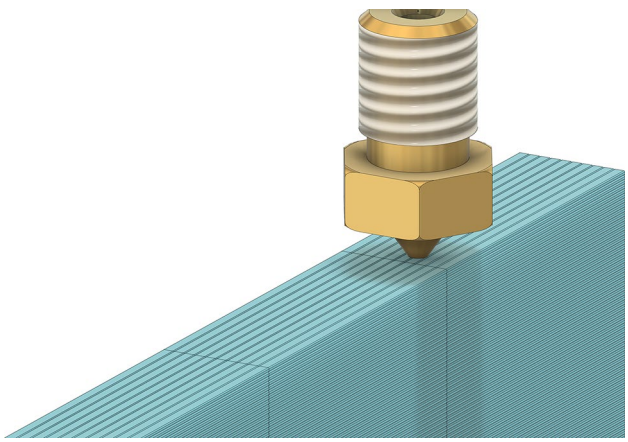

Fig. 2 Schematic of the sample printing (vertical sample)

3 Results

3.1 Determination of porosity through conventional techniques

Figure 4 depicts the variation of the density of the samples produced using different extrusion multipliers and printing orientations. The adoption of higher values of the extrusion multiplier raised the density of both types of samples (vertical and horizontal). However, significant differences between the densities of samples printed with the same extrusion multiplier were observed on samples printed in horizontal and vertical directions. Such difference tended to decrease with higher values of the extruder multiplier; then, a negligible difference was found for the extruder multiplier of 106%. The highest density reached by the printed samples was 1.195 g/mm^3. This value is almost 4.5% lower than the density of the original filament (1.25 g/mm^{-3}) and has a relative density of 95.5%.

Figure 5 depicts the cross-sections made on samples produced by different extrusion multipliers (EMs). The comparison of the cross-sections confirms a gradual reduction of the porosity dimension (darker regions) as the extruder multiplier increases. The porosities were diamond-like, as shown in the higher magnifications reported in Fig. 5. For EM = 94%, the average diagonal of the porosities was 180 mm, while for the samples made with EM = 103% and EM = 106%, the average diagonal was 85 mm.

The analysis of the cross-section enabled us to determine other defects. Samples made using a low extrusion multiplier (EM = 94%) showed a coalescence of porosities in different sample regions. In addition, several unconnected filaments were observed owing to the lower material flow. Such defects were not observed in samples made by higher extrusion multipliers (EM ≥ 97%).

An uneven distribution of the porosities also characterized all the cross-sections. For low extrusion multiplier, the

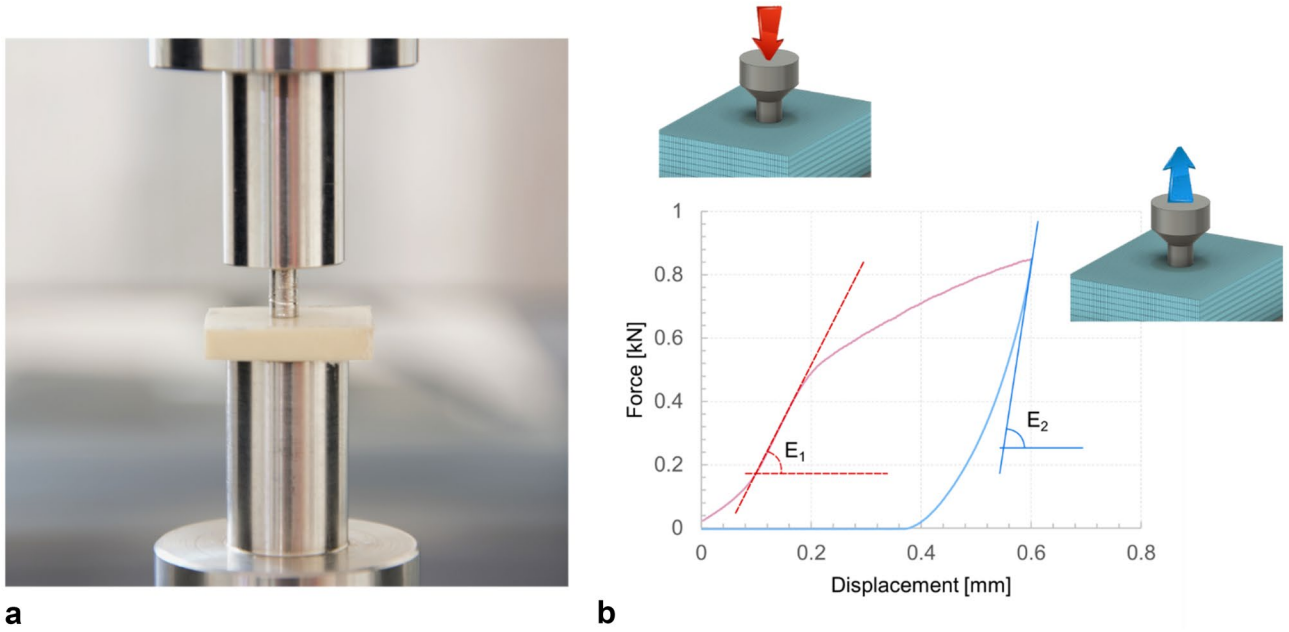

Fig. 3 **a** Experimental equipment and sample orientation during the indentation test; **b** schematic of the force–displacement curve recorded during loading (red) and unloading (blue) phases

variability of the porosity dimension led to the presence of coalescent porosities; on the other hand, in samples printed with higher extrusion multipliers, the outer shells generally showed smaller porosities than those observed in the central region.

3.2 Indentation tests

Figure 6a and b depict the influence of the extrusion multiplier on the slopes E_1 and E_2 (during the loading and unloading phases, respectively) measured through indentation tests using the two indenters ($D=2$ mm and $D=4$ mm, respectively) on samples printed horizontally. The trends indicate a linear increase in the slope with the extrusion multiplier.

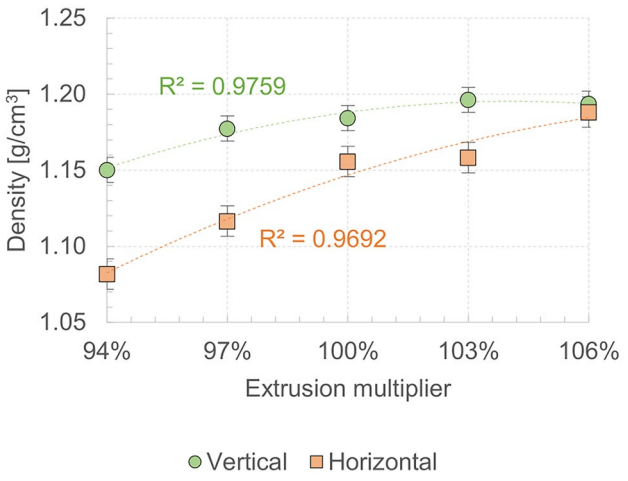

Fig. 4 Influence of the extrusion multiplier and direction of printing on the density of printed samples

However, all the testing conditions (performed with the two indenters and during the loading or the unloading phases) indicated a saturation phenomenon. Indeed, the slopes determined on samples printed with the extrusion multiplier EM = 106% showed a negligible variation compared to those measured on samples printed with EM = 103%.

Figure 7a and b depict the trends of the slopes E_1 and E_2 measured (with indenter diameters $D=2$ mm and $D=4$ mm respectively) on samples printed in the vertical direction. In this case, the tests conducted with the tool diameter $D=4$ mm indicate a non-linear increase of the slopes with the extrusion multiplier characterized by a high coefficient of correlation. This non-linear behavior reflects that determined for the density (shown in Fig. 4). On the other hand, the slope measured through the smaller indenter ($D=2$ mm), as shown in Fig. 7b, was affected by higher uncertainty and dispersion (lower R^2 values).

Cross-correlation among the calculated slopes and the density measurements was performed to determine the best procedure and indenter diameter for density evaluation. Figure 8a depicts the trends of the slopes E_1 and E_2 by different indenter diameters ($D=2$ mm and $D=4$ mm) for horizontal samples. The slope showed a high coefficient of

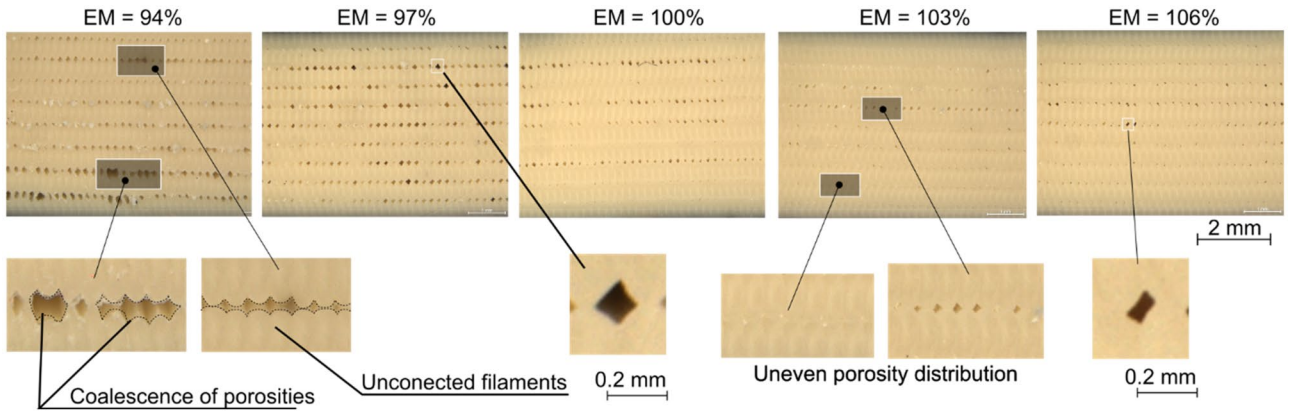

Fig. 5 Cross-sections of vertically printed samples using different extrusion multipliers

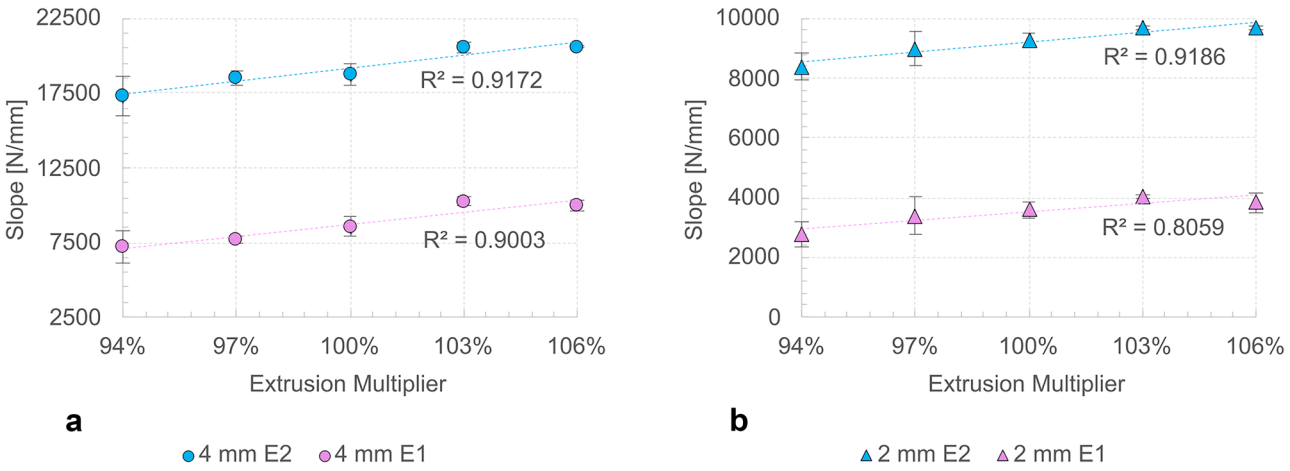

Fig. 6 Influence of the extrusion multiplier on the slope measured during indentation tests on samples printed in **a** $D = 4$ mm and **b** $D = 2$ mm on horizontally printed samples, as schematized in Fig. 3b

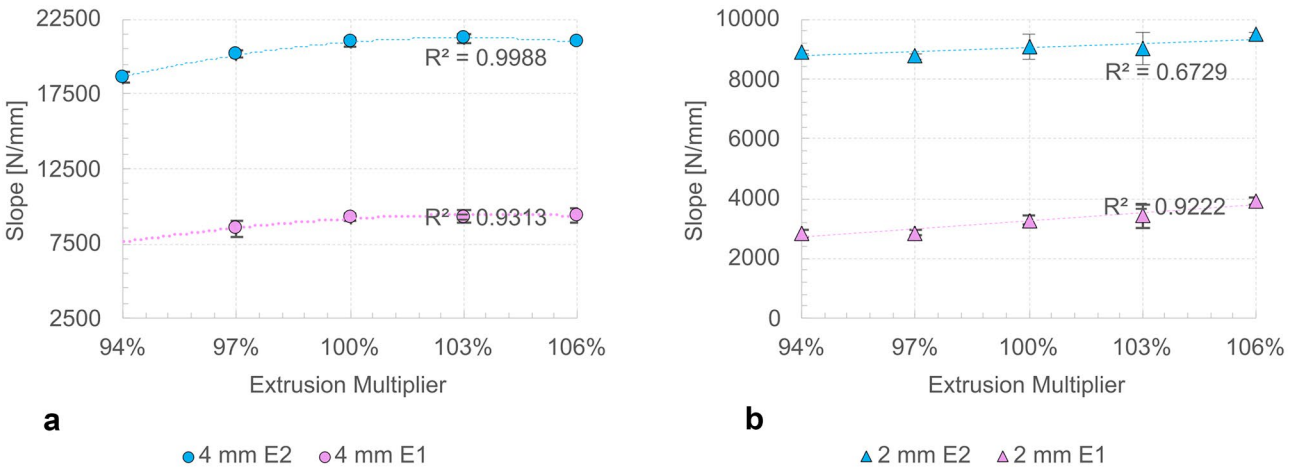

Fig. 7 Influence of the extrusion multiplier on the slope measured during indentation tests on samples printed in **a** $D = 4$ mm and **b** $D = 2$ mm on vertically printed samples

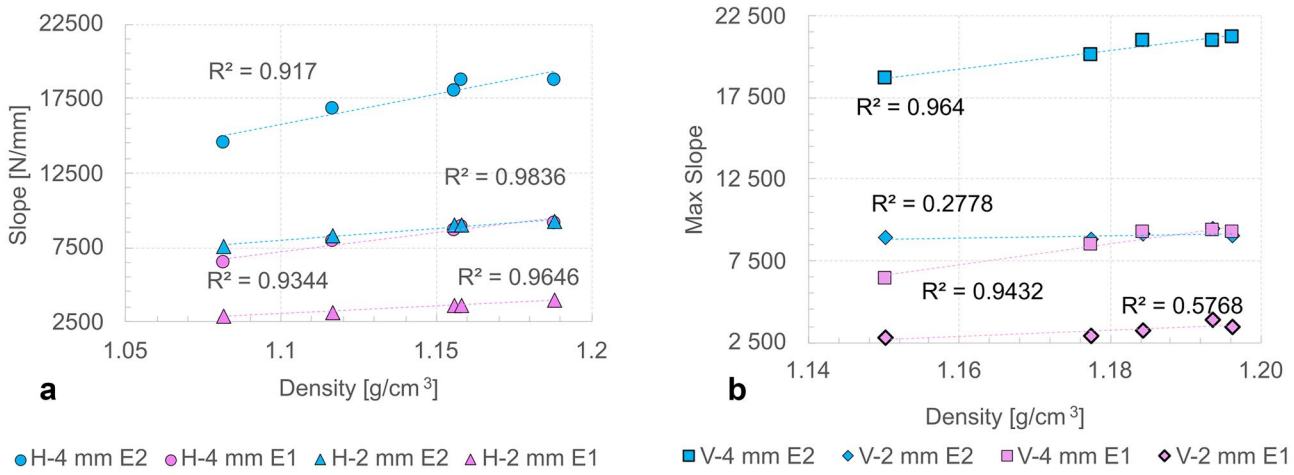

Fig. 8 Correlation of the slopes measured during indentation tests and the density on **a** horizontally printed and **b** vertically printed samples

correlation R^2 in all the testing conditions. The correlation between the slopes and the density for horizontally printed samples ranged between $R^2 = 0.917$ and $R^2 = 0.98$. Figure 8b depicts the correlation between the slope and the density measured on samples printed vertically. In this case, adopting the indenter of $D = 4$ mm confirms a good correlation between the slope and the density; conversely, low values of R^2 for $D = 2$ mm indicate the limit of the smaller indenter for samples printed vertically.

Figure 8a and b indicate the possibility of correlating the slopes of indentation tests with density measurements performed on samples printed in the same direction, in horizontal and vertical directions, respectively. A further cross-correlation analysis was conducted to verify if a relationship can be established between the samples' slopes and density regardless of the printing direction. This analysis was limited to the indenter with $D = 4$ mm since the low values of the coefficient of correlation are shown in Fig. 8b. The relatively high values of the coefficient of correlation as reported in Fig. 9 ($R^2 \approx 0.90$) indicate the reliability of such a general relationship between the slopes and the density of the samples.

3.3 Surface analysis of the printed specimens

The surfaces to be tested during the indentation tests were analyzed to understand better possible causes that led to unreliable test results (especially for the smaller indenter). Figure 10a depicts the 3D surface reconstruction of a sample printed in a vertical direction with the extrusion multiplier set to EM = 100%. The deposited filaments can be clearly distinguished on the surface. The average distance between the filaments is 0.2 mm, corresponding to the layer height adopted in the 3D-printing deposition. Figure 10c depicts a virtual cross-section of the surface which enables to determine better the irregularities of the external surface (that is tested during indentation tests of samples printed vertically). Red dots in Fig. 10c highlight the height of the external filaments. The height of the filaments is comprised between 8 and 30 mm; thus, the surface shows a variation of 22 mm in the surface that is in contact with the indenter. The total roughness R_t value calculated as the difference between the peak surface and the bottom valley is 59 mm. This morphology is consistent with that shown in [14, 15].

The same analysis was performed on the top surface of the samples printed horizontally with an extrusion multiplier EM = 100%, as depicted in Fig. 11. Such surface was even less regular as compared to that observed on the vertical side shown in Fig. 10. Indeed, the maximum peak to valley

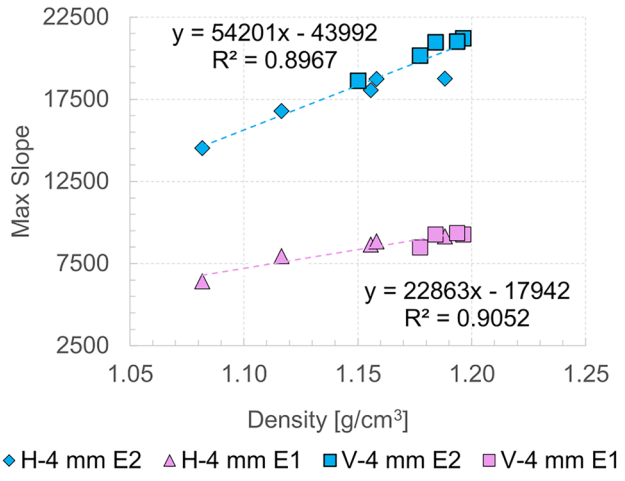

Fig. 9 Overall correlation between the slope measured the indentation tests on horizontal and vertical samples during loading (E_1) and unloading (E_2) phases

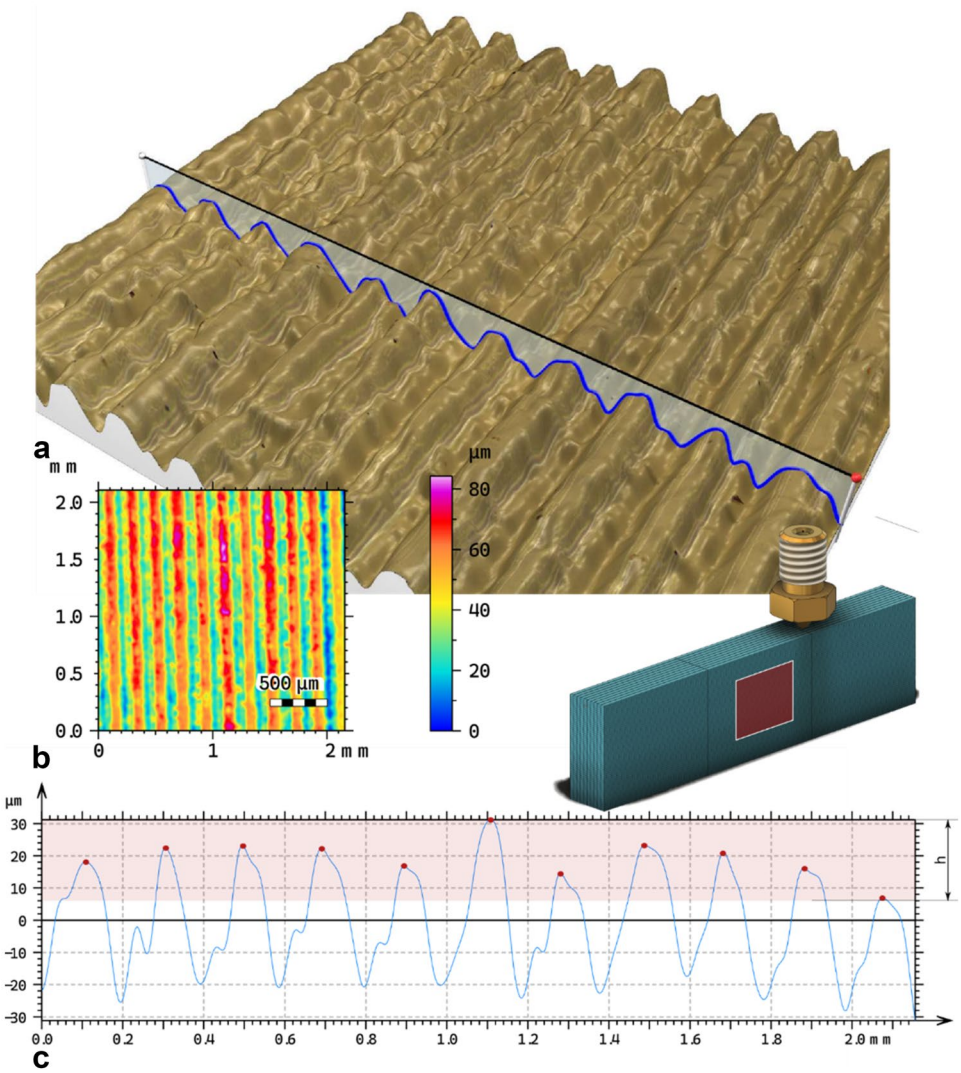

Fig. 10 **a** 3D surface reconstruction of a vertical printed sample; **b** topography of the analyzed surface area; **c** virtual cross-section of the surface

height of the profile Rz is 110 mm. Such a value corresponds to almost half of the layer thickness.

3.4 Influence of deposition strategy

External shells are typically deposited first during the deposition of a layer using fused deposition modeling; then, the process proceeds towards the inner shells. Thus, different deposition conditions are experienced depending on the position of the distance from the external layer perimeter. Figure 12 depicts a schematic of the other deposition conditions occurring during the layer formation with different colors. As mentioned above, the outer layers were first deposited. Therefore, during the deposition of the external shells, barreling edges were produced. Inner shells were deposited differently. Indeed, the material flow of the inner shell was partially constrained by the presence of the filaments already deposited. Therefore, barreling was hindered from the side in contact with the already deposited layer. This was perpetrated as going towards the layer core until the last layer was deposited. Here, the last filament was constrained from both sides, leading to a different material flow than previously deposited filaments. The other deposition conditions lead to an uneven porosity distribution, as depicted in Fig. 12c.

Such porosities participate differently when testing horizontal and vertical samples. Indeed, as schematized in Fig. 13a, during the indentation tests of vertically printed samples, the tool plunges into the barreled side of the external shells. According to the sample orientation, all types of shells (outer to the inner) were loaded during the indentation. On the other hand, during the indentation of the horizontally printed samples, the tool plunged the top (flat) surface of the sample, and only the inner shells were loaded. Figure 13 depicts a schematic of vertical and horizontal samples. While testing vertically printed samples, the load is spread (vertically) over all "types" of deposition (shells with different colors). On the other hand, during indentation tests

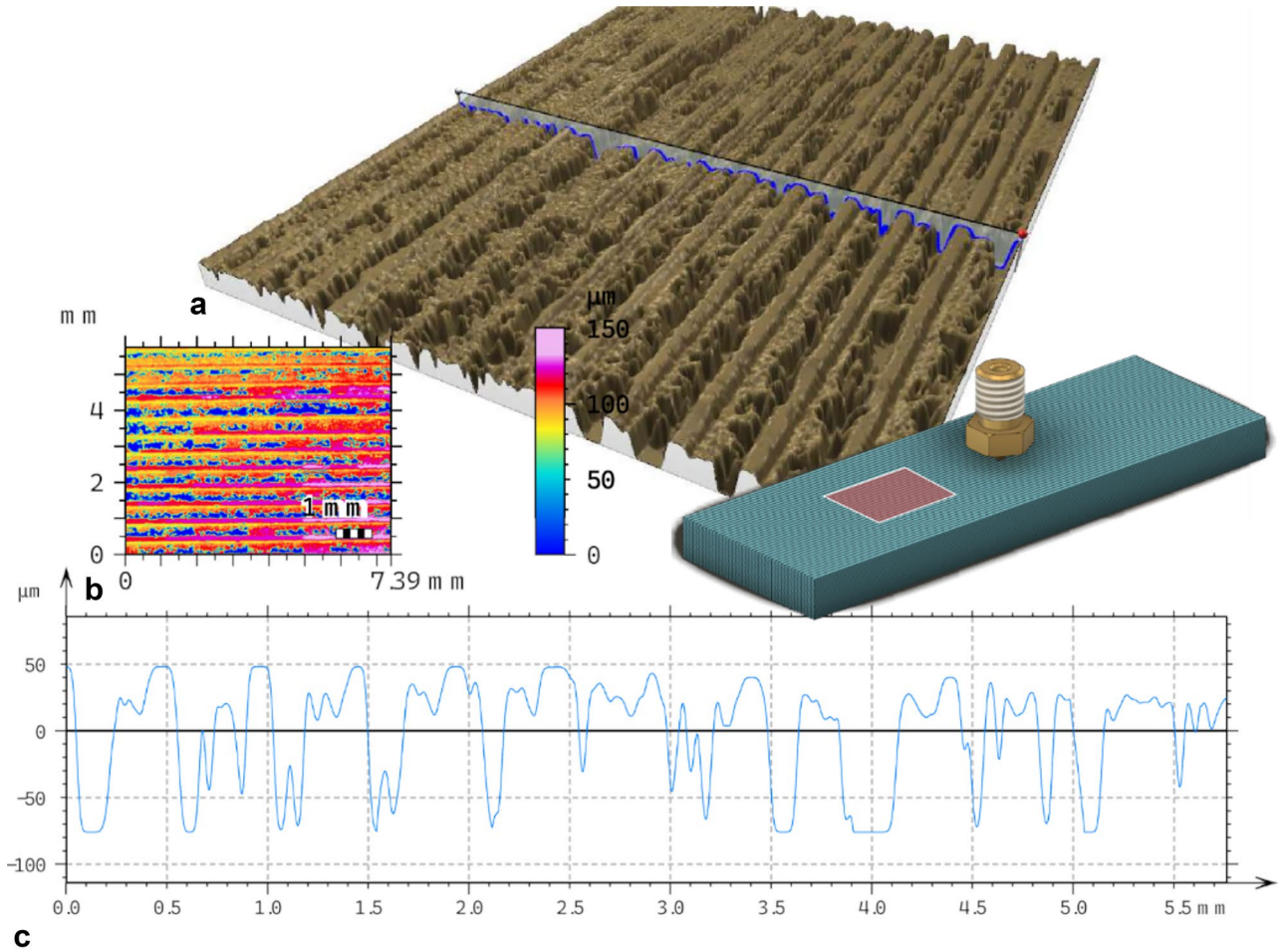

Fig. 11 **a** 3D surface reconstruction of a horizontal printed sample; **b** topography of the analyzed surface area; **c** virtual cross-section of the surface

of the horizontal test, the external shells do not contribute to balancing the load exerted by the indenter.

4 Discussion

Additive manufacturing is a suitable alternative to conventional manufacturing processes in many fields. This is due to several advantages, including the possibility of producing highly customizable products, economic suitability for small batches (even unit batches), extreme geometrical flexibility, distributed production, on-demand production, shortening of the supply chain, and the possibility of continuously improving a component performance with real-time feedback.

However, the adoption of AM processes to produce finished components is still hindered by limitations. Among them, the mechanical characterization is particularly complex on AM products. This is due to a higher sensitivity to the shape and dimensions of the component being produced. Indeed, fixed process parameters and a different temperature history (due to differences in the form, dimensions, local filling, deposition strategy, acceleration/deceleration of the printing head, etc.) may induce significant differences in the local properties of the component. This also makes the development of a testing specimen representative of the element more complex. On the other hand, non-destructive testing can overcome these limitations by providing information on the specific component. This also reduces material waste and does not increase the production time needed for building a series of specimens or physical twins.

Even though the weight and volume measurement can be used to determine the density of the components, this approach is not suitable for complex shapes. In addition, as mentioned above, the density of a component is also highly influenced by the geometry; consequently, the average density cannot be representative of the local properties. On the other hand, the cross-sectioning approach of the actual part is unfeasible. Indeed, it is a destructive method, which would

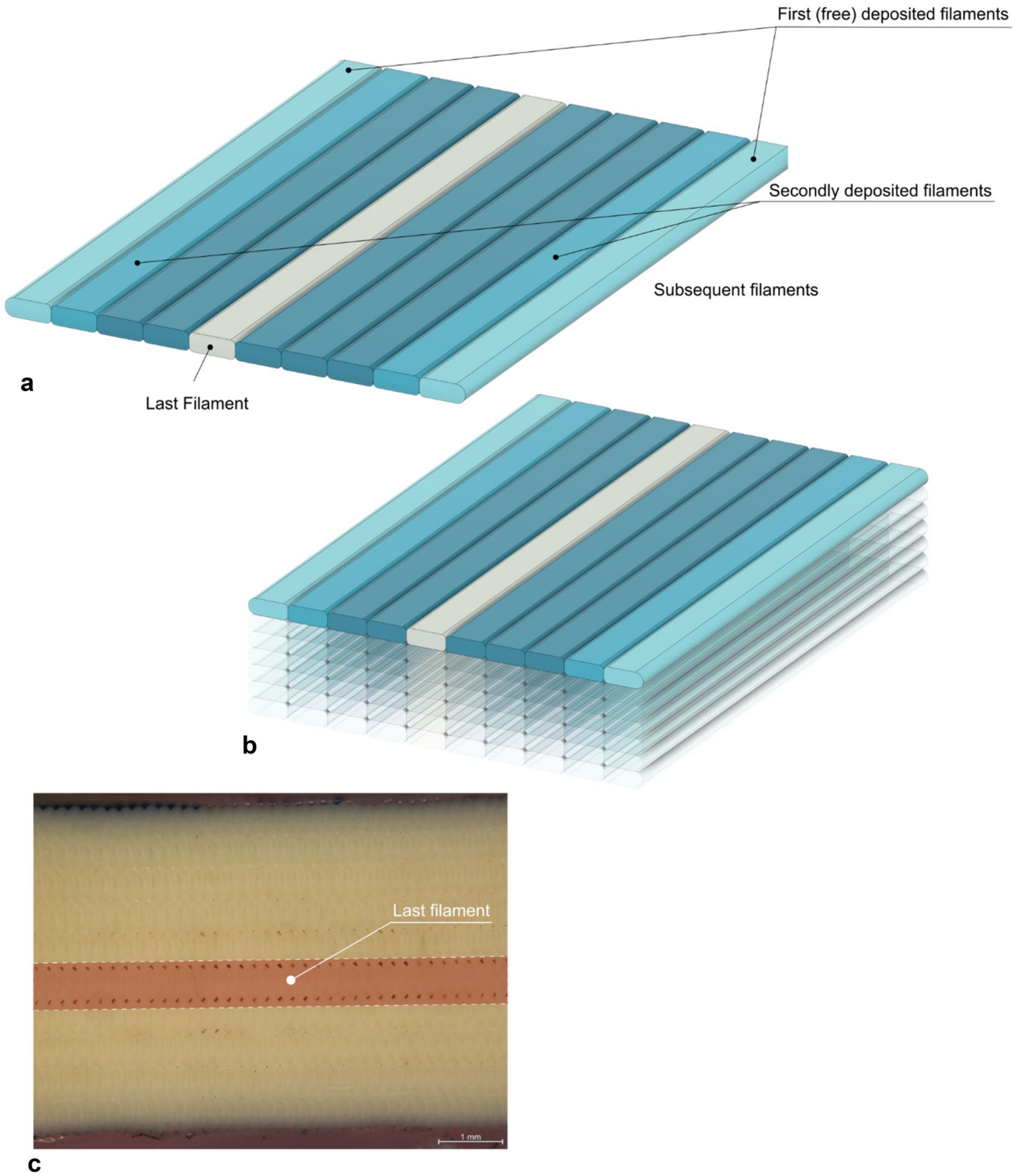

Fig. 12 **a** Schematic of the different material flow conditions arising during the deposition of subsequent shells as moving from the outside perimeter shells towards the core of the layer and **b** during the deposition of subsequent layers; **c** uneven porosity distribution in the central zone

require a physical twin of the actual component to be used for cross-sectioning. This would lead to a significant waste of material and production time. In addition, observations of the porosities through optical microscopy are highly time-consuming since it involves different phases, including cutting, molding, lapping, ultrasonic cleaning to remove possible material flowing within the voids, and optical observation. Consequently, also, this approach is not suitable for

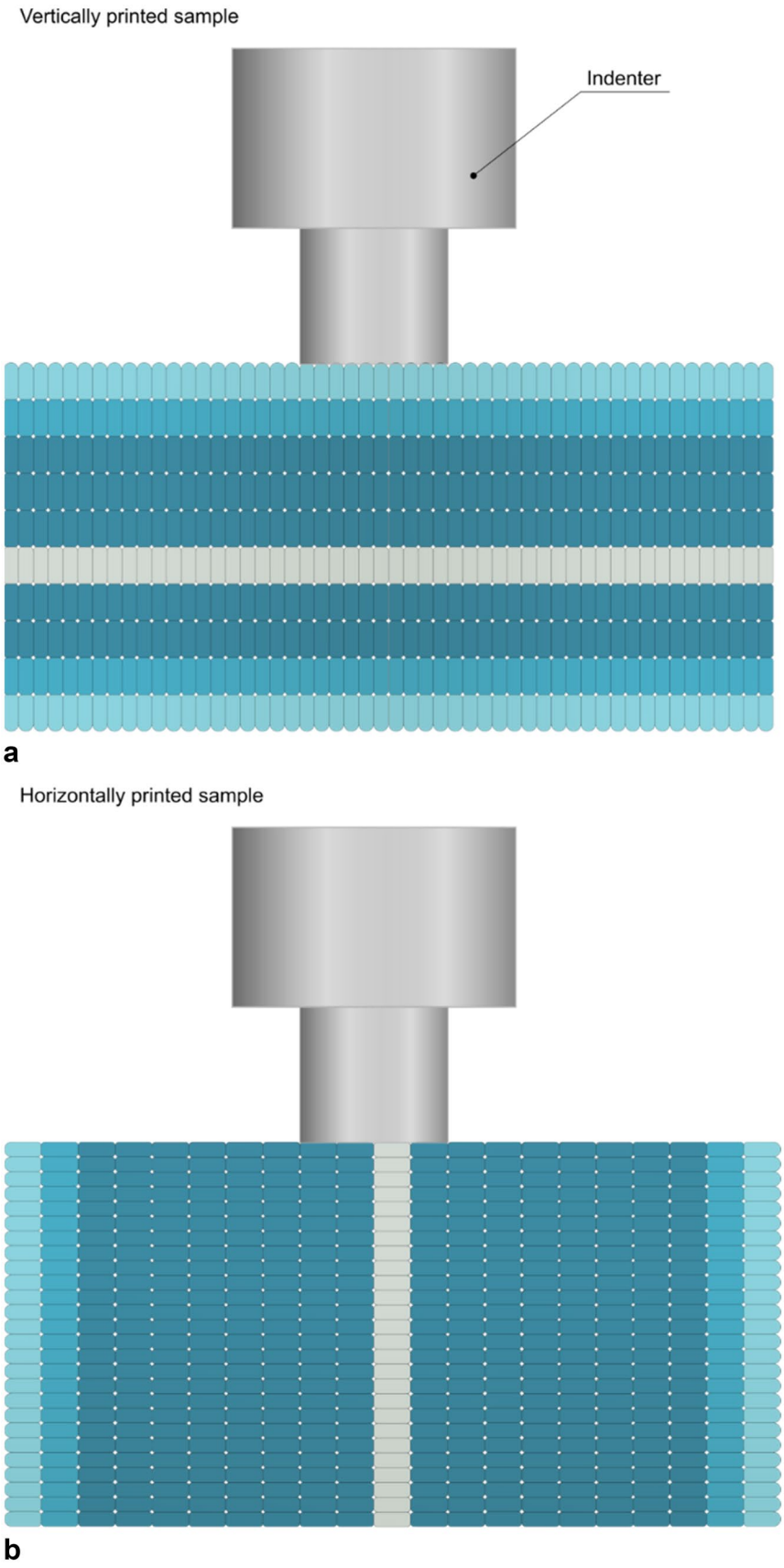

Fig. 13 Schematic of the loaded shells tested during indentation tests on **a** vertically and **b** horizontally printed samples

the needs of production. On the other hand, X-ray computed tomography analysis produces a digital twin of the actual part. However, the application of this method is limited since the cost of the equipment, long scanning time, and the maximum dimension of the part being tested.

The force–displacement features determined during instrumented indentation tests showed a high correlation with the components' density, regardless of the direction of testing. Indeed, both the horizontally printed samples and those printed vertically were successfully characterized through indentation tests. The test performed on horizontally printed samples indicated a high correlation between the force–displacement curves and the porosity measurements regardless of both the tool diameters used in the indentation tests ($D=2$ mm and $D=4$ mm). The correlation coefficient on these samples ranged between $R^2=0.93$ and $R^2=0.98$ depending on the measurement procedure (during the loading and unloading phases) and the tool diameter. On the other hand, when testing the vertically oriented samples, the adoption of the larger tool is mandatory. Indeed, the tests conducted by the smaller indenter ($D=2$ mm) resulted in a weak correlation between the characteristic indentation slopes and the density (R^2 was lower than 0.6). On the other hand, the correlation between the force–displacement slopes and the porosity using the indenter with $D=4$ mm were $R^2=0.94$ and $R^2=0.96$ (in loading and unloading phases, respectively). Thus, even in the presence of internal singularities (such as the presence of connected porosities found on samples printed with a low extrusion multiplier), uneven distribution of the porosities (which were larger in the inner shells), and a rough contact surface between the tool and the indented surfaces, the results from indentation tests showed high correlation with the porosity of the components. This indicates the excellent capability of the proposed methodology to determine the local properties of the components. The tests and the online elaboration of the curves were relatively short (almost 30 s). This indicates the possibility of adopting the test for the quality assessment of finished products.

5 Conclusions

The present investigation proved the suitability of instrumented indentation tests to determine the density of components made by fused deposition modeling (FDM). An experimental campaign was conducted to produce specimens with different porosities. The samples were analyzed using weight and dimensional measurements and image analysis on the cross-sections. The information from other tests was compared to verify the suitability of the proposed methodology. Indentation tests were performed using cylindrical tools of different diameters. The influence of the sample orientation during the tests was also assessed. The main results from the study are reported as follows:

1. The increase in the material flow during 3D printing led to an increase in the specimen's density. This tended to saturate for extrusion multiplier higher than 103%; higher values of extrusion multiplier led to a negligible variation of the density. The samples printed in a horizontal direction showed lower density than those printed vertically. Thus, the printing direction also influences the density of the samples. The highest relative density measured on samples with the highest material flow was 95.5%.
2. Cross-sectional analysis showed a gradual reduction of the porosities with increasing the extrusion multiplier. The porosities had a diamond shape whose longer diagonal reduced from 180 mm (for EM = 94%) to 85 mm (for EM = 103% and 106%). The cross-sections showed variable dimensions of the porosities regardless of the adopted extrusion multipliers. For EM = 94%, the reduced material flow led to the coalescence of porosities in several regions. In samples made with higher material flow conditions, the external shells showed higher density than the inner shells. This was due to the different deposition conditions arising during the layer formation.
3. For horizontally printed samples, the characteristic slopes of the force vs. the displacement curves (measured during the indentation tests) and the density showed a high coefficient of correlation, regardless of the diameter of the indenter. The R^2 values were higher than 0.93 and showed a maximum coefficient of correlation of $R^2=0.98$ (using the tool with 2 mm of diameter during the unloading phase).
4. For vertically printed samples, the smaller indenter ($D=2$ mm) was not suitable for determining the density since poor correlation coefficient. Nevertheless, the correlation coefficient between the density and the slopes measured on force–displacement curves using the larger indenter ($D=4$ mm) was much higher ($R^2=0.96$).
5. Despite the severe difference between the loaded regions and the tested surfaces of horizontally and vertically printed samples, an overall correlation (with $R^2=0.90$) between the slope of the force–displacement curve and the density of the samples was identified.

Funding Open access funding provided by Università degli Studi dell'Aquila within the CRUI-CARE Agreement.

Data availability Not applicable.

Declarations

Ethical approval Not applicable.

Consent to participate Not applicable.

Consent for publication Not applicable.

Competing interests The authors declare no competing interests.

References

1. Li B et al (2022) Electron beam freeform fabrication of NiTi shape memory alloys: crystallography, martensitic transformation, and functional response. Mater Sci Eng A 843:143135
2. Ke WC et al (2022) Multi-layer deposition mechanism in ultra high-frequency pulsed wire arc additive manufacturing (WAAM) of NiTi shape memory alloys. Addit Manuf 50:102513
3. Rodrigues TA et al (2022) Steel-copper functionally graded material produced by twin-wire and arc additive manufacturing (T-WAAM). Mater Des 213:110270
4. Liao Y, Liu C, Coppola B, Barra G, Di Maio L, Incarnato L, Lafdi K (2019) Effect of porosity and crystallinity on 3D printed PLA properties. Polymers (Basel) 11(9)
5. Domingo-Espin M, Puigoriol-Forcada JM, Garcia-Granada A-A, Llumà J, Borros S, Reyes G (2015) Mechanical property characterization and simulation of fused deposition modeling polycarbonate parts. Mater Des 83:670–677
6. Al-Maharma AY, Patil SP, Markert B (2020) Effects of porosity on the mechanical properties of additively manufactured components: a critical review. Mater Res Exp 7 (12)
7. Wang X, Zhao L, Fuh JYH, Lee HP (2019) Effect of porosity on mechanical properties of 3D printed polymers: experiments and micromechanical modeling based on X-ray computed tomography analysis. Polymers (Basel) 11(7)
8. Jin Y, Walker E, Heo H, Krokhin A, Choi T-Y, Neogi A (2020) Nondestructive ultrasonic evaluation of fused deposition modeling based additively manufactured 3D-printed structures. Smart Mater Struc 29(4)
9. Butt J, Bhaskar R, Mohaghegh V (2022) Non-destructive and destructive testing to analyse the effects of processing parameters on the tensile and flexural properties of FFF-printed graphene-enhanced PLA. J Compos Sci 6(5)
10. Alisafaei F, Han C-S (2015) Indentation depth dependent mechanical behavior in polymers. Adv Condens Matter Phys 2015:1–20
11. Schneider-Maunoury C, Albayda A, Bartier O, Weiss L, Mauvoisin G, Hernot X, Laheurte P (2020) On the use of instrumented indentation to characterize the mechanical properties of functionally graded binary alloys manufactured by additive manufacturing. Mater Today Commun 25
12. Zhou Y, Tang Y, Hoff T, Garon M, Zhao FY (2015) The verification of the mechanical properties of binder jetting manufactured parts by instrumented indentation testing. Procedia Manufacturing 1:327–342
13. Farah S, Anderson DG, Langer R (2016) Physical and mechanical properties of PLA, and their functions in widespread applications - a comprehensive review. Adv Drug Deliv Rev 107:367–392
14. Pandey PM, Reddy NV, Dhande SG (2003) Improvement of surface finish by staircase machining in fused deposition modeling. J Mater Process Technol 132:323–331
15. Lambiase F, Genna S, Leone C (2020) Laser finishing of 3D printed parts produced by material extrusion. Opt Lasers Eng 124:105801